Multi-modal safety analysis of the more electric aircraft starter generator system

Z Zeng¹, Y Hu¹, Y Xiong¹, Q Gong², X Xu², H Ge¹*

1. College of Civil Aviation, Nanjing University of Aeronautics and Astronautics, China

2. AVIC China Aero-Polytechnology Establishment, Beijing, China

ABSTRACT

Aiming at the characteristics of complex structure, strong coupling and different multi-modal safety levels of more electric aircraft starter generator system, a safety analysis method based on the operating process and a multi-modal failure rate calculation method are proposed. This paper analyses the architecture, operating process and modals of more electric aircraft starter generator system and decomposes the system into eight operating modals. Based on the construction of SafetyLab, a domestic safety analysis platform, the structural models and failure rate calculation models of eight modals of starter generator system are established, and the top event failure rate of each modal, the highest transient failure rate and the steady state failure rate of the system are calculated for a complete safety analysis, taking a typical starter generator system as an example. The method proposed in this paper helps to solve the problem of multi-modal failure rate analysis of complex systems with different equipment involved in the operating process. The multi-modal failure rate calculation method proposed in this paper is also applicable to the safety analysis of other multi-modal complex systems.

1. INTRODUCTION

To fulfil all the emission and fuel consumption requirements while also meeting those for aircraft safety, new architectures are needed. Currently, the most popular alternative that researchers are working on from a range of perspectives is the more electric aircraft initiative [1-3]. At present, most researchers believe that the safety level of more electric aircraft can be improved by increasing component redundancy. However, some researchers also use algorithms to evaluate the performance of power systems and provide the best power supply path for the load to avoid safety issues [4].

The more electric aircraft starter generator system is closely related to the aircraft functions of ground take-off, in-flight start and electricity generation during cruise. Once the system fault, it will affect flight safety directly [5-6]. As a key technology for more electric aircraft, starter generator system research is relatively lagging behind in China. Current research focus on the control and performance optimization of starter generator system [7-10], while little research pays attention to the safety analysis. Therefore, there is an urgent need to utilize scientific, reasonable, and efficient system safety analysis methods for design optimization of starter generator system, while accumulating experience for the development of domestic more electric aircraft.

*Corresponding Author: allenge@nuaa.edu.cn

The methods used for system safety analysis include Failure Mode, Effects and Criticality Analysis (FMECA) [11], Bayesian Network (BN) [12], Markov Analysis (MA) [13] and Fault Tree Analysis (FTA) [14] and so on. The FTA is a typical qualitative and quantitative safety analysis method, which has been widely used in the safety analysis of aircraft oxygen system [15], flight control system [16], landing gear system [17] and other systems. However, the traditional FTA relies on manual modeling and calculation. For systems with complex structures and functions such as starter generator system, there are problems such as low efficiency, complex modifications, and heavy workload. Therefore, it is necessary to use the relevant safety analysis platform to assist in modeling. Existing safety analysis platforms with FTA functionality come mainly from Europe and the USA, such as Isograph reliability analysis software developed by Isograph company in the UK, and ITEM and Relex software developed in the USA. However, the application of such foreign software would risk technical blocking and information leakage. SafetyLab is a completely domestic safety analysis platform, with the advantages of rich functionality, easy operation and low hardware requirements, which can better solve the problems of low work efficiency, as well as avoid the risk of technical blocking and information leakage.

This paper analyzes the architecture and operating process of more electric aircraft starter generator system comprehensively. Based on the differences in safety levels of each operating mode, the system is decomposed into eight safety analysis modals. Based on the SafetyLab platform developed by members of our group, the multi-modal safety models of the system are established. This paper also establishes the multi-modal failure rate calculation models of the starter generator system, which the various safety indicators of the system are calculated. The results show that the starter generator system meets the safety requirements.

2. OPERATING PRINCIPLE OF THE MORE ELECTRIC AIRCRAFT STARTER GENERATOR SYSTEM

2.1. Architectural of the starter generator system

The more electric aircraft starter generator system is located in two parts: the main engine and the Auxiliary Power Unit (APU) [18]. During normal aircraft operating, the Variable Frequency Starter Generator (VFSG) is used as the core motor of the system for the main engine, usually powered by the APU, while the APU Starter Generator (ASG) is used as the core motor of the system for the APU, usually powered by the external power. Both the VFSG and ASG are three-stage starter generators with similar architectural and function. Figure 1 illustrates the overall architecture of the more electric aircraft starter generator system.

The starter generator system consists of a Main Generator (MG), an Exciter Generator (EG), and a Permanent Magnet Generator (PMG), which form the main body of the system. It's combined with components such as ATRU, CMSC, excitation power circuit, rotating rectifier, and various breakers and contactors to achieve current control and voltage regulation during system operating. The starter generator system can achieve switching between start and generation functions, providing the torque required for engine start and the electric power required for normal aircraft operating.
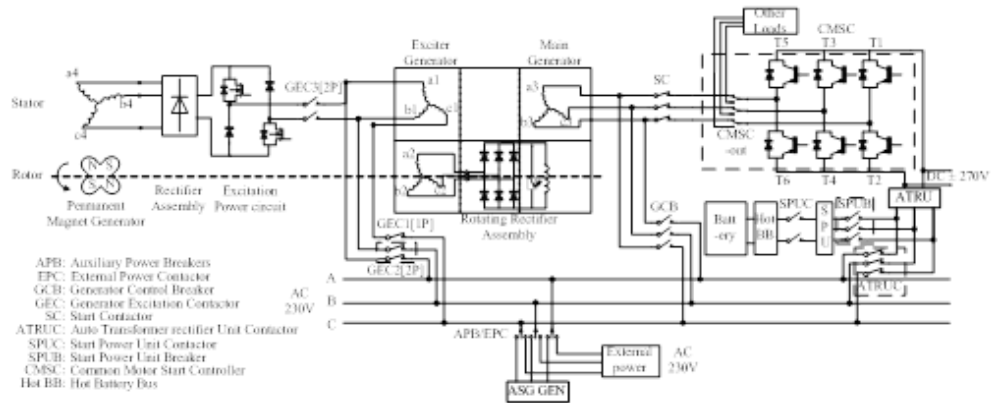
Figure 1: Architectural of the more electric aircraft starter generator system

2.2. Operating modes of the starter generator system

According to the different operating functions of the system, the starter generator system is decomposed into start condition, transition condition, and generation condition. Under different operating conditions, slight differences in the operating of various components within the system can have an impact on the overall safety analysis of the system, so it is necessary to subdivide the operating mode of the system. Table 1 analyzes the operation modes of the starter generator system.

Table 1. Operating modes of the starter generator system

System operating conditions	System operating modes	RPM of engine	Main function of the system
Start condition	3-phase start mode	$0\sim n_1$	Provide start torque
	2-phase start mode	$n_1\sim n_2$	Provide start torque
Transition condition	Transition mode	$n_2\sim n_3$	Rotate coaxially with the engine
Generation condition	Generate mode	$\geq n_3$	Output AC power

In the Tab.1, n_1 represents the maximum RPM for constant torque start, n_2 represents the engine disengagement RPM, and n_3 represents the minimum RPM for engine generation. In the case of the B787, n_1 takes a value of 4000rpm, n_2 takes a value of 6780rpm, and n_3 takes a value of 7200rpm.

The start condition is decomposed into two modes: 3-phase start mode and 2-phase start mode. Figure 2 shows the operating state of the system components for the 3-phase start mode of the starter generator system. At initial start, the RPM of the engine is zero. The system supplies constant frequency and variable frequency 3-phase Alternating Current (AC) to the exciter generator stator winding and main generator stator winding respectively, and the interaction between the rotating magnetic fields drives the rotor RPM of the main generator, thus completing the initial start of the main engine.
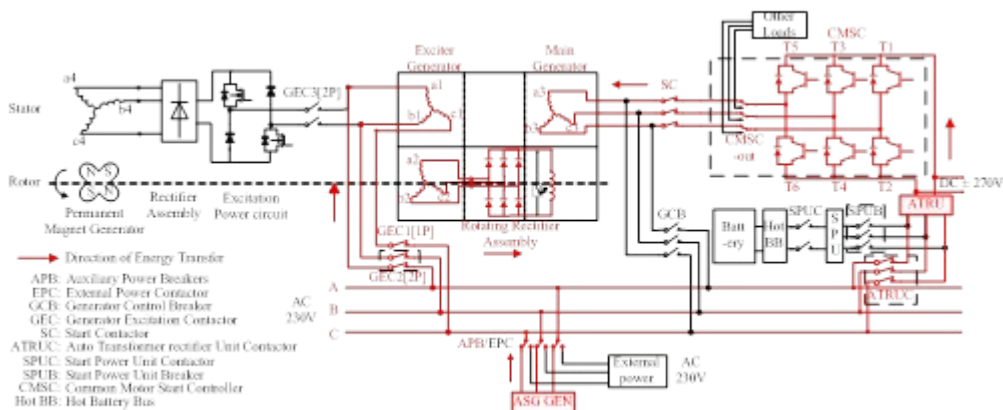
Figure 2: 3-Phase start mode of the starter generator system (RPM of Engine < n_1)

When the engine RPM reaches n_1, theGEC1 is disconnected, and the starter generator system is switched from 3-phase start to 2-phase start. But the main function of the system remains to provide the start torque. When RPM of the engine accelerates to n_2, the starter generator system enters transition mode, at which point the system neither outputs torque nor generates electricity. As the RPM of the engine continues to increase to n_3, the system switches to the generate mode. The stator winding of the main generator cuts the magnetic field of the rotor winding, generating 3-phase AC.

3. MULTI-MODAL SAFETY MODELING PLATFORM AND SOLUTION FOR STARTER GENERATOR SYSTEM

3.1. Safety modelling platform--SafetyLab

SafetyLab, also known as the Accident Dynamic Simulation and Analysis Platform, is a domestic software, which was developed with the participation of our research team. SafetyLab platform has the advantages of rich functionality, easy operation, and low hardware requirements. The system structure models built by SafetyLab can clarify the operating status of each component under different operating modals. When performing fault tree analysis, the models can intuitively reflect the relationship between the bottom events and the system architectural. SafetyLab can accurately and efficiently complete the safety analysis research of this paper. Figure 3 displays the operation interface of SafetyLab.

3.2. Multi-modal division of the starter generator system

On the one hand, there are differences in the operation of the components in the different operating modals of the system; on the other hand, the starter generator system has high requirements for the transient switching performance of the operating modes during operation. Therefore, it is necessary to conduct safety analysis of switching transient and process states between various operating modes of the starter generator system. Before conducting safety modeling, the four modes mentioned above can be divided into eight safety analysis modals. Figure 4 illustrates the eight modals of the starter generator system.
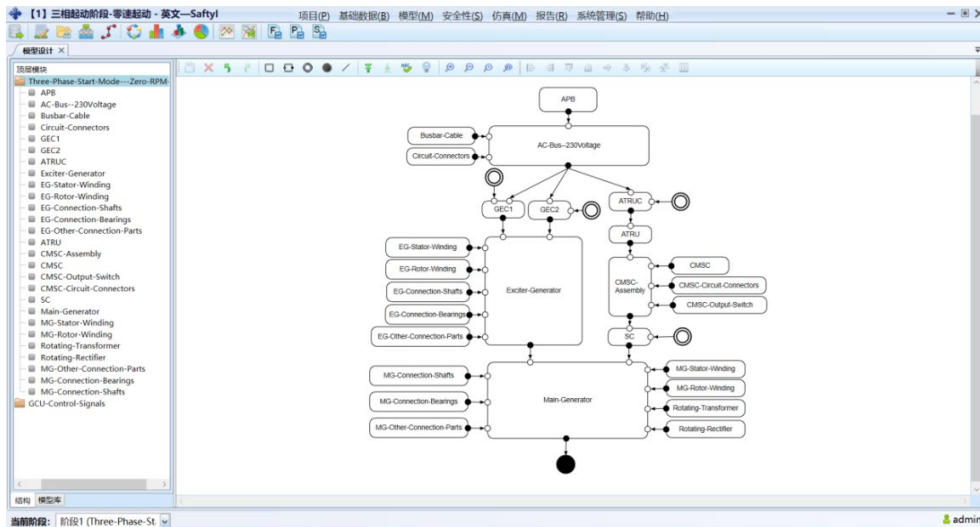
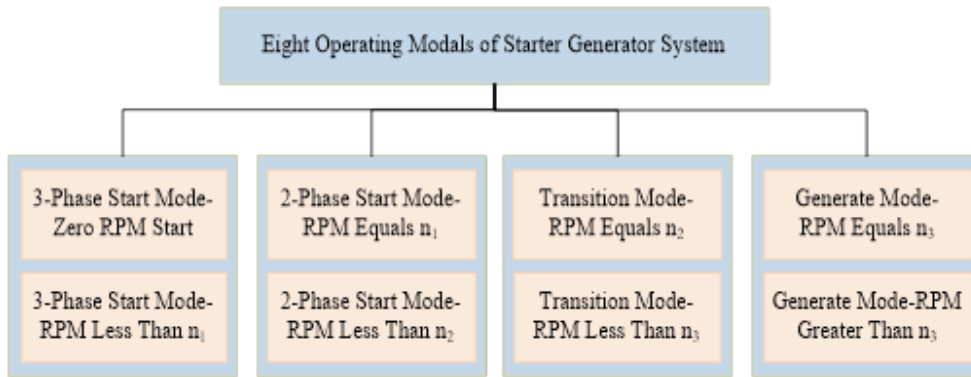Figure 3: Operation interface of the domestic software SafetyLab

Figure 4: Eight safety analysis modals of the starter generator system

4. CONSTRUCTION OF THE MULTI-MODAL SAFETY MODELS OF THE STARTER GENERATOR SYSTEM

4.1. Multi-modal structural modelling of the starter generator system

This paper uses the SafetyLab platform to construct structural models of eight operating modals of the system. Selecting two typical modals: "3-Phase Start Mode - Zero RPM Start" and "Transition Mode - RPM Equals n_2" to introduce the specific modeling process.

4.1.1. System structure model of "3-Phase Start Mode - Zero RPM Start" modal

At the "3-phase start mode - zero RPM start" modal, the Generator Control Unit (GCU) controls the on-off of components such as GEC1, GEC2, ATRUC and SC. Therefore, whether the GCU can correctly issue contactor control signals will also have an impact on the safety level of the operating modal of "3-phase start mode - zero RPM start". Figure 5 shows the first layer of the structural model of the system in this modal.
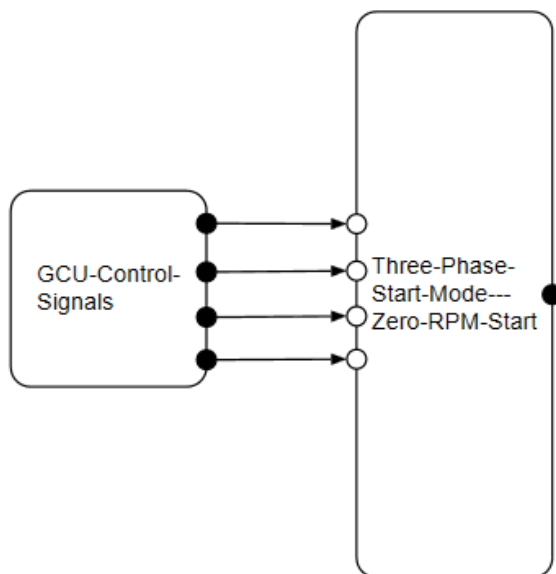
Figure 5: The first layer of the SafetyLab model for "3-Phase Start Mode - Zero RPM Start" modal

Within the starter generator system of the main engine in the "3-phase start mode - zero RPM start" modal, APU supplies power to 230V AC bus bar via APB. Then, the AC current being sent to the bus bar will be divided into two current flows. It's one flow direction, 230V 3-phase AC flows through GEC1 and GEC2 into the exciter generator stator winding and generates a pulsating magnetic field around the stator winding. The rotor winding of the exciter generator cuts the magnetic induction lines to produce 3-phase AC. The AC is rectified to Direct Current (DC) by the rotating rectifier and fed to the rotor winding of the main generator, around which a constant magnetic field is formed. In the other flow direction, 230V 3-phase AC flows through the ATRUC into the ATRU. ATRU rectifies AC to 270V DC to supply CMSC. The CMSC further inverts DC power into AC power with controlled current and voltage. The controlled AC will flow through the SC into the stator winding of the main generator and create a three-phase rotating magnetic field around the winding. Finally, the rotating magnetic field interacts with the constant magnetic field, and the main generator outputs the start torque to drive the main engine to rotate. Figure 6 shows the second layer of the structural model of the system in this modal.

4.1.2. System structure model of the "Transition mode - RPM Equals n_2" modal

When the RPM of the main engine reaches n_2, the start mode of the starter generator system ends, the system needs to go through the transition mode from start to generating. In the transient state where the engine RPM equals n_2, the GCU controls the SC and GEC2 disconnection. As the starter generator system is neither generating electricity nor outputting torque at this time, only the motor is required to rotate coaxially with the engine. Therefore, when considering the impact of the exciter generator and main generator on system safety, only the operating state of the mechanical part of the motor and the rotating transformer (RPM measurement) are considered. Figure 7 shows the second layer of the structural model of the system in this modal.
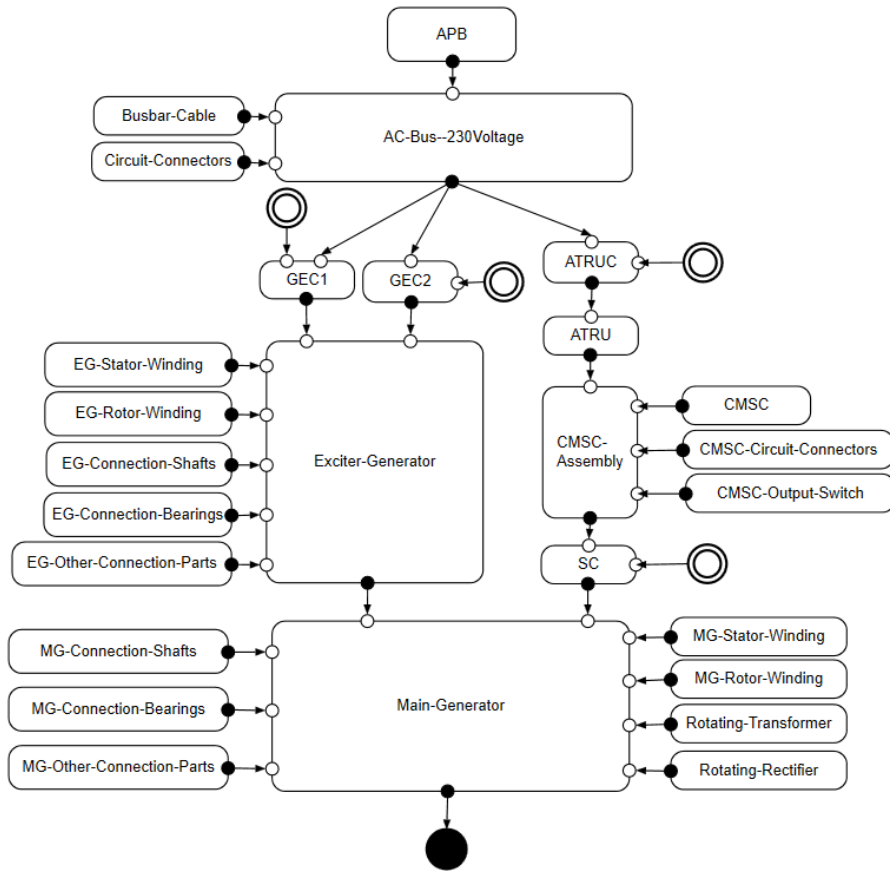
Figure 6: The second layer of the SafetyLab model for "3-phase start mode - zero RPM start" modal
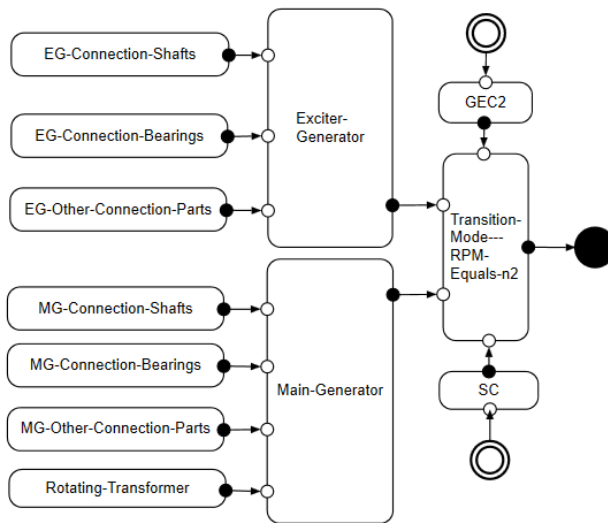

Figure 7: The second layer of the SafetyLab model for "Transition mode - RPM Equals n₂" modal

The FTA bottom events of each modal are shown in Table 2. In the "Modals" column of the table, (1 to 8) represent the eight modals from "3-phase start mode - zero RPM start" to "generate mode - RPM greater than n_3".

Table 2. Correspondence between bottom events and various modals

No.	bottom events (Fault)	Modals	No.	bottom events (Fault)	Modals
F_1	GEC1 Control Signal	(1)(3)	F_{20}	EG Stator Winding	(1)-(4)(7)(8)
F_2	GEC2 Control Signal	(1)(5)	F_{21}	EG Rotor Winding	(1)-(4)(7)(8)
F_3	GEC3 Control Signal	(7)	F_{22}	EG Connection Shafts	(1)-(8)
F_4	SC Control Signal	(1)(5)	F_{23}	EG Connection Bearings	(1)-(8)
F_5	ATRUC Control Signal	(1)	F_{24}	EG Other Connection Parts	(1)-(8)
F_6	GCB Control Signal	(7)	F_{25}	MG Stator Winding	(1)-(4)(7)(8)
F_7	APB	(1)-(4)	F_{26}	MG Rotor Winding	(1)-(4)(7)(8)
F_8	Bus Bar Cable	(1)-(4)(7)(8)	F_{27}	MG Connection Shafts	(1)-(8)
F_9	Circuit Connectors	(1)-(4)(7)(8)	F_{28}	MG Connection Bearings	(1)-(8)
F_{10}	GEC1	(1)(2)(3)	F_{29}	MG Other Connection Parts	(1)-(8)
F_{11}	GEC2	(1)-(5)	F_{30}	Rotating Transformer	(1)-(8)
F_{12}	GEC3	(7)(8)	F_{31}	Rotating Rectifier	(1)-(4)(7)(8)
F_{13}	SC	(1)-(5)	F_{32}	PMG Stator Winding	(7)(8)
F_{14}	ATRUC	(1)-(4)	F_{33}	PMG Rotor Winding	(7)(8)
F_{15}	GCB	(7)(8)	F_{34}	PMG Connection Shafts	(7)(8)
F_{16}	ATRU	(1)-(4)	F_{35}	PMG Connection Bearings	(7)(8)
F_{17}	CMSC	(1)-(4)	F_{36}	PMG Other Connection Parts	(7)(8)
F_{18}	CMSC Circuit Connectors	(1)-(4)	F_{37}	GCU Rectifier Bridge	(7)(8)
F_{19}	CMSC Output Switch	(1)-(4)	F_{38}	GCU Excitation Power Circuit	(7)(8)

5. CALCULATION OF THE MULTI-MODAL FAILURE RATE FOR STARTER GENERATOR SYSTEM

5.1. Failure data analysis

In order to calculate the top event failure rate of each modal, it's necessary to first obtain the failure rate data of each bottom event. In this paper, it's assumed that the failure rate of each bottom event follows an exponential distribution.

Investigate the MIL-HDBK-217F [19] "Electronic Equipment Reliability Projections" manual and review the failure rate data of various components in the system. As an example, the failure rate of the circuit breaker components such as the GCB and APB in the starter generator system is calculated as,

$$\lambda_P = \lambda_b \pi_C \pi_U \pi_Q \pi_E \tag{1}$$

in equation (1), λ_P is the failure rate of the bottom event component, λ_b is the fundamental failure rate, and π_C, π_U, π_Q and π_E represent the structure factor, application factor, quality factor and environment factor respectively. Substituting the data gives $\lambda_{PGCB} = 0.1122 \times 10^{-6}/h$ and $\lambda_{PAPB} = 0.2805 \times 10^{-6}/h$.

The failure rate calculation model of rotating transformer is shown in equation (2) below,

$$\begin{cases} \lambda_P = \lambda_b \pi_N \pi_E \\ \lambda_b = 0.00535 \, exp(\frac{T_C+273}{334})^{8.5} \\ T_C = 40°C + T_E \end{cases} \tag{2}$$

in equation (2), π_N and π_E represent the brush quantity factor and environment factor. T_C and T_F represent the Component temperature and Environmental temperature. Substituting the data gives $\lambda_{PRT} = 0.3584 \times 10^{-6}/h$.

For bottom events for which failure rate data is not available by consulting reliability manuals or specifications, the failure rate data can be estimated using an analogous factor approach, i.e. by multiplying the failure rate data of other similar bottom events by the failure rate correction factor,

$$\lambda_P = \lambda_G K_F \tag{3}$$

in equation (3), λ_G is the failure rate of the similar component, K_F is the correction factor. For civil aircraft application components, K_F is generally taken as 25 to100. The estimated failure rate of each control signal transmission in the system is $\lambda_{PSignal} = 0.005 \times 10^{-6}/h$ (optical cable length 10m, K_F taken as 50).

The bottom event failure rate for each modal is obtained or estimated by the two methods described above. See Tab.3.

Table 3. Failure rate of the bottom events

No.	Failure rate λ_{Pi} $(10^{-6}/h)$	No.	Failure rate λ_{Pi} $(10^{-6}/h)$	No.	Failure rate λ_{Pi} $(10^{-6}/h)$
F_1	0.0050	F_{10}	0.1247	F_{19}	0.3480
F_2	0.0050	F_{11}	0.1870	$F_{20\sim24}$	0.1520
F_3	0.0050	F_{12}	0.1870	$F_{25\sim29}$	0.1520
F_4	0.0050	F_{13}	0.1122	F_{30}	0.3584
F_5	0.0050	F_{14}	0.1122	F_{31}	0.0851
F_6	0.0050	F_{15}	0.1122	$F_{32\sim36}$	0.1520
F_7	0.2805	F_{16}	0.3330	$F_{37\sim38}$	0.0864
F_8	0.1500	F_{17}	0.2826		
F_9	0.4224	F_{18}	0.1056		

To facilitate data interpretation, F_{20} to F_{24} are unified as EG fault: F_{20-24}, F_{25} to F_{29} are unified as MG fault: F_{25-29}, F_{32} to F_{36} are unified as PMG fault: $F3_{2-36}$, and F_{37} to F_{38} are unified as generator rectifier control faults F_{37-38}.

5.2. Calculation of failure rate for starter generator system

5.2.1. Top event failure rate of each modal

The bottom events of each modal are independent of each other, and each bottom event occurring causes the top event to occur. Therefore, the failure rate λ_{Pi} of relevant components can be summed to obtain the top event failure rate λ_i of each modal, see Eq. (4). Table 4 calculates the top event failure rate for each modal.

$$\lambda_i = \lambda_{P1} + \lambda_{P2} + \ldots + \lambda_{Pn} \tag{4}$$

Table 4. Top event failure rate of each modal

Modals	λ_i $(10^{-6}/h)$	Modals	λ_i $(10^{-6}/h)$
3-Phase Start Mode - Zero RPM Start	3.2257	Transition Mode - RPM Equals n_2	0.8500
3-Phase Start Mode - RPM Less Than n_1	3.2057	Transition Mode - RPM Less Than n_3	0.4508
2-Phase Start Mode - RPM Equals n_1	3.2107	Generate Mode - RPM Equals n_3	1.8675
2-Phase Start Mode - RPM Less Than n_2	3.0810	Generate Mode - RPM Greater Than n_3	1.8575

5.2.2. Maximum transient failure rate of the system

The system failure rate for each operating modal of the starter generator system is calculated in section 5.2.1 above. See Eq. (5). The results show that the "3-Phase Start Mode - Zero RPM Start" modal has the maximum transient failure rate λ_{smax}.

$$\lambda_{smax} = \max (\lambda_1, \lambda_2, \dots, \lambda_n) \tag{5}$$

The λ_{smax} is $3.2257 \times 10^{-6}/h$, which reflecting the most vulnerable state of the starter generator system.

5.2.3. Steady state failure rate of the system

This paper will further analyze the safety level in the steady state of the system. Consider the ratio of the operating time of each modal to the total operating time and calculate the steady state failure rate of the system by weighting and summing the failure rates of each modal.

Researching relevant manuals and materials [20], obtain the total operating time T from start to stable generating and the operating time t_i for each modal of the starter generator system. The steady state failure rate of the system λ_s can be calculated using the following equation (6):

$$\begin{cases} \lambda_s = \sum_{i=1}^{8} \alpha_i \lambda_i \\ \alpha_i = \frac{t_i}{T} \end{cases} \tag{6}$$

The calculation of the system steady state failure rate λ_s is $2.1802 \times 10^{-6}/h$.

Considering the regular inspection and maintenance of civil aircraft in actual operating, calculate the system reliability $R(t = 1000h)$ of single-channel starter generator system in 1000h using equation (7).

$$R(t) = e^{-\lambda_s t} \tag{7}$$

$R(t = 1000h)$ is 0.997822. Calculations show that after 1000h of operating, the reliability of a single-channel starter generator system can still reach over 0.99.

In addition, the electric system of more electric aircraft is a multi-redundant system. Furthermore, this paper calculates the system failure rate of the dual-channel starter generator system after 1000 hours of operation using equation (8).

$$\lambda_{ns}(t) = \frac{n\lambda_s e^{-\lambda_s t}(1 - e^{-\lambda_s t})^{n-1}}{1 - (1 - e^{-\lambda_s t})^n} \tag{8}$$

When n is taken as 2 and t as 1000, $\lambda_{2s}(1000) = 9.4756 \times 10^{-9}$. For civil aircraft, the steady state failure rate of the dual-channel starter generator system after 1000 hours of operation can reach 10^{-9} magnitude, which meets the airworthiness requirements.

6. CONCLUSION

Aiming at the characteristics of complex structure, strong coupling and different multi-modal safety levels of more electric aircraft starter generator system, a safety analysis method based on the operating process and a multi-modal failure rate calculation method are proposed. The main conclusions are as follows.

i. Taking a typical type of starter generator system as an example, the architecture, operation process and modals of the system are analyzed in detail, and the structural modelling of the eight operating modals is completed based on the domestic safety analysis platform, the system analysis process is reasonable and feasible, and the platform-based auxiliary modelling is efficient.

ii. Propose a multi-modal failure rate calculation method. Calculate the safety indicators such as the top event failure rate of each modal, the highest transient failure rate, and the steady state failure rate. A complete safety analysis is conducted on the system, and the calculation results verified that the typical starter generator system meets the airworthiness safety requirements.

iii. The method proposed in this paper helps to solve the problem of multi-modal failure rate analysis of complex systems with different equipment involved in the operation process. The multi-modal failure rate calculation method proposed in the paper is also applicable to the safety analysis of other multi-modal complex systems.

ACKNOWLEDGMENTS

REFERENCES

[1] Yang Y, & Gao Z., "Power optimization of the environmental control system for the civil more electric aircraft", Energy, 2019, 172: p.196-206.

[2] Garriga, A.G., Govindaraju, P., Ponnusamy, S.S., Cimmino, N., Mainini, L., "A modelling framework to support power architecture trade-off studies for More-Electric Aircraft", Transportation Research Procedia, 2018, 29: p. 146–156.

[3] Talbi, S., Mabwe, A.M., El Hajjaji, A., "A Hierarchical Control of a Li-ion Battery Charger for More Electric Aircraft", IFAC-PapersOnLine, 2017, 50(1): p. 9412–9418.

[4] Rodríguez, F., Martínez, G. A. I. Z. K. A., Rodríguez, S., & Echeverría, J. M., "Increasing the safety of more electric aircraft through a novel algorithm in the DC power system", International Journal of Electrical Power & Energy Systems, 2021, 126(Part A): p. 106566.

[5] Borghei, M., & Ghassemi, M., "Insulation Materials and Systems for More- and All-Electric Aircraft: A Review Identifying Challenges and Future Research Needs", IEEE Transactions on Transportation Electrification, 2021, 7(3): p. 1930-1953.

[6] Apostolidou, N., & Papanikolaou, N., "Active Power Control of Switched Reluctance Generator in More Electric Aircraft", IEEE Transactions on Vehicular Technology, 2021, 70(12): p.12604-12616.

[7] Sarakhanova, R. Y., Zharkov, M. A., & Alexandrov, I. V., "Synthesis of the control algorithm for the parallel voltage inverter as part of the starter-generator system for aircraft", 2022 IEEE 23rd International Conference of Young Professionals in Electron Devices and Materials (EDM), Altai, Russian Federation, IEEE, 2022, p.383-387.

[8] Yang, J.Z., Ouyang, J.P., Chen, X.Y., Meng, F.X., Wang, L., Liu, L.X., "Review on Design of Electric Environment Control System for More Electric Aircraft", Advances in Aeronautical Science and Engineering, 2022, 13(4): p.11-24.

[9] Sedky, M. M., Abdel-Azim, W. E., Abdel-Khalik, A. S., & Massoud, A. M., "Integrated Switched Reluctance Starter/Generator for Aerospace Applications: Particle Swarm Optimization for Constant Current and Constant Voltage Control Designs", Applied Sciences, 2022, 12(15): p. 7583.

[10] Mohamed, M. A., Shen Yeoh, S., Atkin, J., Diab, A. M., Khalaf, M., & Bozhko, S., "Enhanced Starting Control Scheme for PMM - Based Starter / Generator System for MEA", Aerospace, 2023, 10(2): p. 168.

[11] Dabous, S. A., Ibrahim, F., Feroz, S., & Alsyouf, I., "Integration of failure mode, effects, and criticality analysis with multi-criteria decision-making in engineering applications: Part I - Manufacturing industry", Engineering Failure Analysis, 2021, 122: p. 105264.

[12] Kong, X.F., Wang, J., Zhang, Z.M., "Reliability Analysis of Aircraft Electric System Based on Bayesian network and CCF", Acta Aeronautica et Astronautica Sinica, 2020, 41(05): p. 270-279.

[13] Accardi, L., Lu, Y. G., & Souissi, A., "A Markov-Dobrushin Inequality for Quantum Channels", Open System & Information Dynamic, 2021, 28(4): p. 2150018.

[14] Fazlollahtabar, H., & Niaki, S. T. A., "Fault tree analysis for reliability evaluation of advanced complex manufacturing system", Journal of Advanced Manufacturing Systems, 2018, 17(1): p.107-118.

[15] Zhang, D.X., Guo, J.L., "Dynamic fault tree analysis of an aircraft oxygen system", Aviation Maintenance and Engineering, 2021, (07): p.57-59.

[16] Chung, E., & Hanks, J. S., "Fault Tree Analyses as a Tool for Flight Control System Architecture Design", 2016 Annual Reliability and Maintainability Symposium (RAMS), Tucson, AZ, USA, IEEE, 2016, p. 1-6.

[17] Armaan, A., Keshav, S., & Srinivas, G., "A step towards safety: Material failure analysis of landing gear", Materials Today: Proceedings, 2020, 27(Part 1): p.402-409.

[18] Hamilton Sundstrand, Boeing 787 Electrical System. REPORT: Hamilton Sundstrand. 2011.

[19] Department of Defense, MIL-HDBK-217F, Reliability prediction of electronic equipment. STANDARD: Washington DC: Department of Defense. 1990.

[20] Wu, Z.M., Ge, H.J., Hu, Y.X., Pan, S.Y., Jin, H., Sang, Y.Q., "Failure Correlation Analysis of More Electric Aircraft Starter Generator System Based on DEMATEL", Measurement and Control Technology, 2022, 41(10): p.32-37.